

## Density dependence of the electron surface barrier for fluid $^3\text{He}$ and $^4\text{He}$ †

James R. Broomall

*Department of Physics, University of Delaware, Newark, Delaware 19711  
and Department of Physics, Lincoln University, Pennsylvania 19352*

Wayne D. Johnson

*Department of Physics, University of Delaware, Newark, Delaware 19711*

David G. Onn

*Department of Physics and Division of Health Sciences, University of Delaware, Newark, Delaware 19711*

(Received 14 July 1975; revised manuscript received 5 January 1976)

The density dependence of the electron surface barrier for  $^3\text{He}$  and  $^4\text{He}$  fluids has been determined by injection of electrons from a planar gold surface into the liquid and the dense vapor phases. Barrier values for both isotopes are consistent with a Wigner-Seitz calculation for atomic densities up to the experimental limit of  $1.8 \times 10^{22} \text{ cm}^{-3}$  ( $^3\text{He}$ ) and  $3.0 \times 10^{22} \text{ cm}^{-3}$  ( $^4\text{He}$ ). Comparison of results with other theoretical and experimental values is presented.

### I. INTRODUCTION

It has been recognized for some time now that the short-range repulsive exchange interaction between an electron and a helium atom gives rise to two related phenomena for electrons interacting with bulk helium. These are (a) the creation of a stable "bubble" state for the electron in dense helium fluid, in which the electron displaces helium atoms from a spherical volume whose radius is dependent on the fluid density, and (b) the existence of an effective potential barrier  $E_B$  at liquid surfaces, which is about 1 eV for the liquid under saturated vapor pressure and which attenuates a current of low-energy electrons entering the fluid. In the present work we have determined  $E_B$  for both helium isotopes over a wider range of densities than has previous been possible, enabling us to observe the density dependence of  $E_B$ , and to distinguish between applicable theoretical models.

Several theoretical calculations of  $E_B$  have been made in the past<sup>1-5</sup> and will be reviewed in Sec. II. Previous experimental determinations of  $E_B$ ,<sup>6-10</sup> which are discussed in Sec. V, have encountered at least one of two limitations. Either the experimental analysis required use of the parameters of the "bubble" model, or the experiment did not permit measurements to be made over a large range of densities owing to the requirement for a free helium surface. In contrast, our own results are obtained at a planar gold surface, provided by a thin-film cold-cathode electron source, which permits a wide range of densities to be achieved, not only in the liquid, but also in the vapor phase over a wide temperature range.

Our new injection results are both more precise and more consistent than earlier injection studies

of helium.<sup>11,12</sup> It is the combination of these improved results with a knowledge of the energy distribution of the injected electrons that enables us to obtain consistent values of the electron surface barrier, rather than analyzing the results in terms of an assumed barrier as in previous work.

### II. SURVEY OF THEORETICAL BARRIER CALCULATIONS

Various models have been used to calculate the density dependence of the electron-helium surface barrier. In this section we review four of these models, which we later compare with our experiments.

(a) The earliest approach by Lenz using an optical approximation predicts that the barrier  $E_B$  is given by<sup>2</sup>

$$E_B = 2\pi\hbar^2 na / m_e, \quad (1)$$

where  $a$  is the electron-helium scattering length and  $n$  is the atomic number density of the helium. We refer to this result as OM below.

(b) An extension of this approach by Fetter<sup>3</sup> includes the two-body correlation function  $g(r)$ , and leads to the following expression for  $E_B$ :

$$E_B = \frac{2\pi\hbar^2 na}{m_e} \left( 1 - na \int \frac{g(r) - 1}{r} d^3r \right). \quad (2)$$

If  $g(r)$  is approximated by a step function

$$g(r) = \begin{cases} 0, & r \leq r_s \\ 1, & r > r_s \end{cases}$$

where  $\frac{4}{3}\pi nr_s^3 = 1$ , expression (2) above becomes

$$E_B = (2\pi\hbar^2 na / m_e)(1 + 2\pi nar_s^2). \quad (3)$$

We refer to this approach as the modified optical model (MOM).

(c) An alternative approach<sup>4</sup> uses a Wigner-Seitz calculation considering the helium as a periodic array of hard spheres each of radius  $a$ , and a Wigner-Seitz equivalent sphere radius  $r_s$ . This leads to a condition for the minimum wave number for propagation of the electron in the lattice as

$$k_0 r_s = \tan[k_0(r_s - a)].$$

Barrier values are then calculated from

$$E_B = \hbar^2 k_0^2 / 2m_e. \quad (4)$$

This model is referred to below as WSM.

(d) Tankersley<sup>5</sup> makes use of available structure-factor data to calculate the barrier values as a function of temperature and pressure at liquid densities, using the form

$$E_B = \frac{2\pi\hbar^2 na}{m_e} \left( 1 + \frac{2a}{\pi} \int_0^\infty S(l) dl \right), \quad (5)$$

where  $S(l)$  is the static structure factor for helium. This can be carried out in the density range  $1.7 \times 10^{22} < n < 2.2 \times 10^{22} \text{ cm}^{-3}$ . For  $n > 2.2 \times 10^{22} \text{ cm}^{-3}$  where no structure-factor data are available, he uses the MOM [Eq. (3)] to compute  $E_B$ , while at densities less than  $1.7 \times 10^{22} \text{ cm}^{-3}$  he assumes an effective hard-core radius  $b$  and uses a predicted correlation function<sup>5</sup> to yield

$$E_B = (2\pi\hbar^2 na/m_e) \left\{ 1 + 2\pi nab^2 \left[ 1 - \left( \frac{11}{30} \pi \right) nb^3 \right] \right\}. \quad (6)$$

A comparison of these calculations, using  $a = 0.63 \text{ \AA}$  for the electron-helium scattering length, is shown in Fig. 1. The prime determining factor for the barrier height is the atomic density  $n$ , while temperature effects appear to be negligible on this scale. However, the density dependence of the barrier is clearly different in each of the

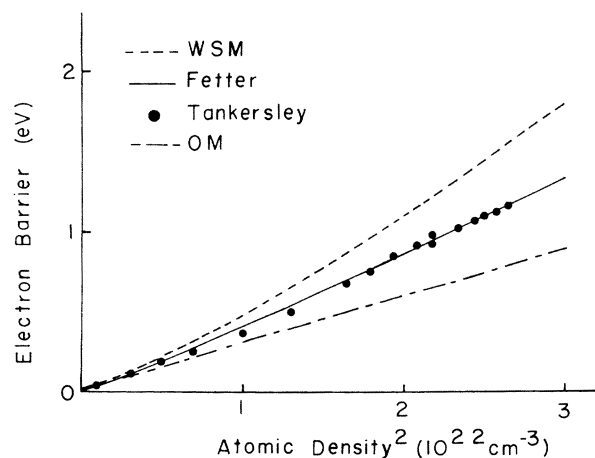


FIG. 1. Theoretical barrier predictions for four models. Tankersley's two methods yield slightly different results at an atomic density of  $2.2 \times 10^{22} \text{ cm}^{-3}$ . See text for references.

models, except that the results of Tankersley and the MOM are in close agreement.

In Sec. IV we will compare our experimental results for the density dependence of the barrier height with the predictions of the WSM and the MOM.

### III. EXPERIMENTAL PROCEDURES

The primary experimental measurement is the attenuation of an electron current injected into pure samples of the two helium isotopes,  $^3\text{He}$  and  $^4\text{He}$ , at various densities. The electron source is a thin-film cold-cathode emitter which provides electrons with known energy distribution, with an average energy about 1 eV.

The experimental arrangement is similar to that used in previous electron injection experiments.<sup>11-13</sup> A planar gold-plated collector is mounted 0.025 cm from the electron emitter, allowing fields up to 60 000 V/cm to be applied to the helium samples. The fabrication and the operational details of the electron emitters, which have an Al-Al-oxide-Au structure, as well as the retarding grid method used to obtain their energy distribution have been described elsewhere.<sup>14</sup> Care was taken to always operate the emitters in the "temperature-independent mode," ensuring a known reproducible electron energy distribution. In addition, data-taking techniques were standardized and accurately timed in order to account for the unavoidable emitter "aging." The precautions taken resulted in data that were reproducible, even for different emitters, to better than  $\pm 5\%$ . This is a marked improvement over previous injection data.

The emitter-collector combination was mounted in a stainless-steel pressure cell mounted in a temperature-controlled cryostat, covering the range from 1.5 to 100 °K. Collected current was monitored by a Keithley 616 digital electrometer, floating up to 1200 V, enabling currents down to  $10^{-14} \text{ A}$  to be measured. Temperature was determined from a Cryocal<sup>15</sup> calibrated germanium thermometer, and controlled electronically. The high-purity gas samples<sup>16</sup> were pressurized with a stainless-steel nitrogen-trapped mercury Toeppler pump and delivered to the pressure cell through a 0.11-cm-i.d. stainless-steel tube. After reaching thermal and pressure equilibrium the sample pressure was determined from one of two Heise<sup>17</sup> pressure gauges.

Densities for  $^4\text{He}$  as a function of temperature and pressure were taken from the data of McCarty.<sup>18</sup> Liquid densities for  $^3\text{He}$  were obtained from the data of Sherman and Edeskuty.<sup>19</sup> For  $^3\text{He}$  vapor above 4.2 °K, the density was obtained by a virial expansion using the second and third virial coefficients of Keller.<sup>20</sup>

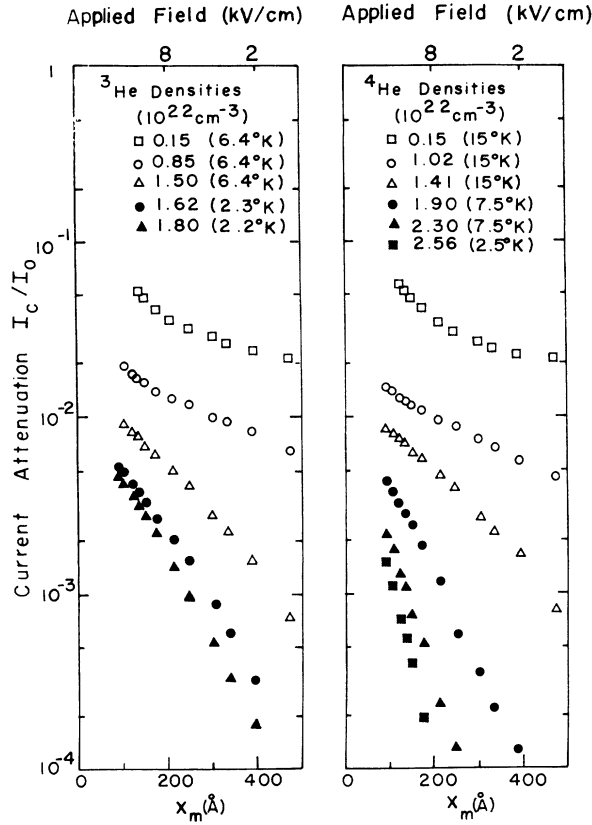


FIG. 2. Typical collected current data for  ${}^3\text{He}$  and  ${}^4\text{He}$  at various temperatures and atomic density. Analysis includes data out to  $x_m \cong 1000 \text{ \AA}$ .

#### IV. EXPERIMENTAL RESULTS AND DATA ANALYSIS

In a previous paper<sup>2</sup> it was shown that, at low temperatures and high densities, the injected current attenuation follows the form

$$I_c/I_0 = (A/D)e^{-x_m/x_0}, \quad (7)$$

where  $I_c$  is the collected current with helium sample present,  $I_0$  is the collected current in vacuum,  $x_0$  is the electron thermalization distance in the fluid, and  $x_m = (e/16\pi\epsilon_0\mathcal{E})^{1/2}$  is the distance to the potential peak arising from the combined electron image field and the sample applied field  $\mathcal{E}$ .  $D$  describes the back diffusion of the unthermalized injection electrons, and  $A$  describes the effect of the electron-helium surface barrier; both terms are discussed in more detail below. While Eq. (7) only applies when thermalization is very rapid, it provides a useful form for presenting our experimental data.

$$\frac{I_c}{I_0} = \frac{A}{D} \left(1 + \frac{kT}{e\mathcal{E}x_0}\right)^{-1/2} \left( K_1 \left\{ \left[ \frac{e^2}{4\pi\epsilon kT} \left( \frac{1}{x_0} + \frac{e\mathcal{E}}{kT} \right) \right]^{1/2} \right\} / K_1 \left[ \left( \frac{e}{kT} \frac{e\mathcal{E}}{4\pi\epsilon} \right)^{1/2} \right] \right). \quad (9)$$

$K_1(x)$  is most readily evaluated in terms of a polynomial expansion in powers of  $x$ . In particular, for

In Fig. 2 we show typical attenuated-current characteristics obtained for  ${}^3\text{He}$  and  ${}^4\text{He}$  at a variety of densities plotted in the form of Eq. (7). It can be seen that for high densities and low temperatures the form of Eq. (7) is followed quite accurately, and that values of  $A/D$  and  $x_0$  can be obtained directly. At higher temperatures and lower densities a more complete analysis is necessary, and is outlined below.

To describe electron injection into dense argon, nitrogen, and hydrogen gases, Smejtek *et al.*<sup>13</sup> have developed a model, which we now apply to the helium isotopes, treating the injected electrons as a two-component fluid consisting of thermalized and unthermalized electrons. Utilizing continuity of current and appropriate boundary conditions, a differential equation results, which may be solved analytically by an approximation referred to as the strong diffusion approximation (SDA). The solution for the electron yield becomes

$$\frac{I_c}{I_0} = \frac{\exp(x_s/x_0)}{D} \times \frac{\int_0^\infty \exp(-x/x_0) \exp[eV(x)/kT] dx}{\int_0^\infty \exp[eV(x)/kT] dx}, \quad (8)$$

where  $x$  is the distance from the emitter and  $-dV(x)/dx = E(x)$ , the combined image and applied electric fields, is valid when

$$x > \frac{[1 + (64\pi\epsilon E_0/e^2)x_0]^2 - 1}{32\pi\epsilon E_0/e^2},$$

where  $E_0$  is the injection energy.

We note that the previous application of the SDA was limited to cases where either the surface electron barrier did not exist or had a minimal attenuation effect compared to other factors. The presence of the helium fluid in front of the electron emitter may be viewed as causing a shift of the electron potential energy by an amount  $E_B$ . Since the barrier affects not only the initial attenuation of the injected electron stream but also the effective energy of the electrons penetrating the fluid, we need to modify this model to explicitly include the effect of the barrier on the yield.  $E_0$  will be interpreted as the net average electron energy above the barrier. The fraction of electrons emitted in vacuum with energy greater than the barrier is designated by  $A$  and introduced in the same manner as in Eq. (7). Since the integrals in Eq. (8) may be evaluated in terms of modified Bessel functions,  $K_1(x)$ , Eq. (8) becomes

$(e/kT)(e/4\pi\epsilon)^{1/2} > 2$ ,  $K_1(x) = x^{-1/2} e^{-x} [1.25 + 0.235(2/x) - \dots]$ . For  $x \gg 2$  Eq. (9) may be approximated as

$$\frac{I_c}{I_0} = \frac{A}{D} \left( 1 + \frac{kT}{\epsilon \mathcal{E} x_0} \right)^{-1} \exp \left\{ -\frac{x_m}{x_0} \left[ 1 - \frac{1}{4} \left( \frac{kT}{\epsilon \mathcal{E} x_0} \right) + \frac{1}{8} \left( \frac{kT}{\epsilon \mathcal{E} x_0} \right)^2 + \dots \right] \right\}, \quad (10)$$

when  $kT/\epsilon \mathcal{E} x_0 < 1$ . It is now apparent that the SDA reduces to Eq. (7) which we refer to as the rapid thermalization model when the thermal energy of the thermalized electrons is too small to overcome the applied field ( $kT/\epsilon \mathcal{E} x_0 \ll 1$ ).

The term  $A$  is numerically the fraction of electrons in the original energy distribution with energies greater than the electron surface barrier  $E_B$ , and can be determined directly from the known electron energy distribution in vacuum  $n(E)$ :

$$A = \int_{E_B}^{\infty} n(E) dE / \int_0^{\infty} n(E) dE. \quad (11)$$

This method treats the transmission over the barrier classically, but a more rigorous quantum-mechanical treatment<sup>21</sup> shows no effects observable by our method.

A second effect of the surface barrier is to reduce the average velocity of the injected electrons. The resulting reduced average kinetic energy  $E_0$  is determined by calculating the effect of the barrier  $E_B$  on the known electron energy distribution in vacuum:

$$E_0 = \int_{E_B}^{\infty} (E - E_B) n(E) dE / \int_{E_B}^{\infty} n(E) dE. \quad (12)$$

$E_0$  must be considered in the calculation of the cross sections to be used in the back-diffusion term  $D$  as discussed below.

The back-diffusion term  $D$  which arises naturally in the solution of the SDA had previously been discussed by Thomson as well as Loeb.<sup>22</sup> The general form is

$$D = 1 + K x_0 / x_s, \quad (13)$$

where  $x_s$  is the mean free path for momentum scattering, and  $K$  is a constant which may assume any value from 0.75 to about 2.5 depending on experimental conditions. This wide variation is explained in the SDA in terms of the scattering at one mean free path under the influence of the electron image field. The back-diffusion term  $D$  arises directly as a result of the balance of current applied at  $x_s$  in terms of the injected current density  $j_0$  and  $\rho_h$ , the hot electron charge density:

$$j_0 = \langle -v_x(x_s) \rangle \rho_h(x_s) + \frac{1}{\tau} \int_{x_b}^{\infty} \rho_h(x) dx, \quad (14)$$

where  $\tau$  is the mean thermalization time for the injected hot electrons, and  $\langle -v_x(x_s) \rangle$  is the average velocity component directed back to the emitter

for electrons scattered at  $x_s$  under the influence of the image field. Employing conservation of energy and using the approach due to Thomson,<sup>22</sup> we obtain

$$\langle -v_x(x_s) \rangle = (6\pi)^{-1/2} \left( \frac{2}{m} \right)^{1/2} \left( E_0 + \frac{e^2}{16\pi\epsilon x_s} \right)^{1/2}. \quad (15)$$

This calculation yields a value for  $D$  in the form of Eq. (13) with the term

$$K = \left( \frac{6}{\pi} \right)^{1/2} \left( 1 + \frac{e^2}{16\pi\epsilon x_s E_0} \right)^{1/2}.$$

The value of  $x_s$  is calculated from the electron-helium cross section for momentum scattering  $\sigma_s$  as  $x_s = 1/n\sigma_s$ . This approach differs somewhat from that of Smejtek *et al.*, but differences in the resulting barrier calculations are within our experimental error.

The cross-section values used in describing the back diffusion are based on O'Malley's fit of  $\sigma_m$  to experimental energy-dependent values for low-density helium gas<sup>23</sup> modified by Legler's correction for multiple scattering.<sup>24</sup> At the energies and densities of concern to us it is necessary to include the effects of multiple scattering because the electron wavelength and the mean free path are comparable. At a density of  $1 \times 10^{21} \text{ cm}^{-3}$  the correction is negligible for electrons having an energy of 1 eV; but at a density of  $2 \times 10^{22} \text{ cm}^{-3}$ , there is a 30% effect.

To illustrate the method used in extracting the value of the surface barrier we refer to Fig. 2, showing current attenuation  $I_c/I_0$  against  $x_m$ . At a particular temperature, Eq. (9) implies that a fit to  $x_0$  suffices to determine the curve shape. An initial value of  $E_0$  equal to the average energy of the electron distribution in vacuum is used to calculate  $x_s$ , which combined with  $x_0$  specifies  $D$  and therefore  $A$ . From  $A$  both  $E_B$  and a new value for  $E_0$  may be found using Eqs. (11) and (12), respectively. The new value of  $E_0$  is then iterated until a final value of  $E_0$  is found which is consistent to better than 1% from start to finish, and gives a corresponding consistent value of  $E_B$ .

In practice, Eq. (10) is used where valid for all but the lowest-density data. The low-density data are analyzed by Eq. (9), the results from the two forms agreeing in the overlap region. Preliminary results have been presented elsewhere.<sup>25</sup> Our values for  $E_B$  as a function of atomic density based on more comprehensive data using the analysis above, are shown in Fig. 3 for both  $^3\text{He}$  and  $^4\text{He}$ .

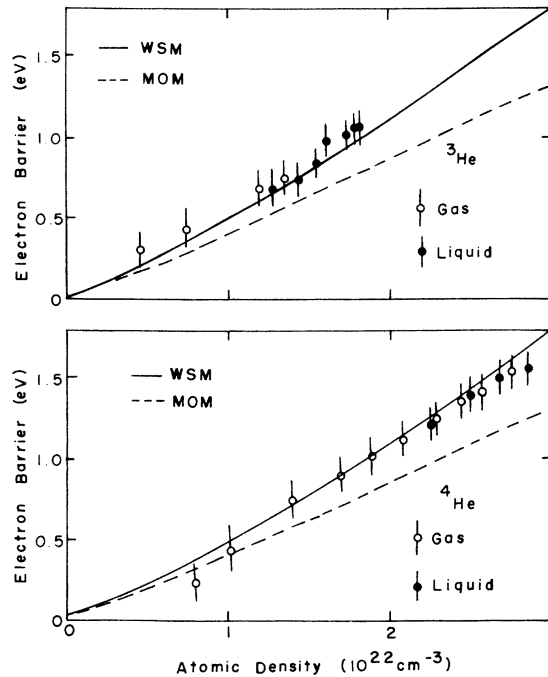


FIG. 3. Experimental barrier values for  ${}^3\text{He}$  and  ${}^4\text{He}$  as a function of atomic density. The  ${}^4\text{He}$  barrier values in the liquid represent multiple points. Experimental error is estimated on the uncertainty in the electron energy distribution and uncertainty in  $x$ .

Values of the injected-electron thermalization time obtained with this analysis are shown in Fig. 4 as a function of density. A least-squares fit to the logarithmic plot shows the thermalization time varying approximately as  $n^\alpha$ , where  $\alpha = -3.1 \pm 0.3$  for  ${}^4\text{He}$  and  $\alpha = -2.1 \pm 0.3$  for  ${}^3\text{He}$ . For the lower atomic densities the electron thermalization time is less for  ${}^3\text{He}$  than for  ${}^4\text{He}$ , suggesting a dependence on the atomic mass. At higher densities, in both gas and liquid, this mass dependence is no longer apparent.

#### V. DISCUSSION

Referring to Fig. 4 we note that our experimental barrier values for  ${}^3\text{He}$  in the range  $1.2 \times 10^{22} < n < 1.8 \times 10^{22} \text{ cm}^{-3}$  and for  ${}^4\text{He}$  for  $8.0 \times 10^{21} < n < 2.9 \times 10^{22} \text{ cm}^{-3}$  show the Wigner-Seitz model to be most consistent with our results. Below an atomic density of  $8 \times 10^{21} \text{ cm}^{-3}$  our experimental uncertainty does not allow a clear distinction between theoretical models to be made.

Table I compares our barrier results with those of previous investigations. Except for the data of Zipfel and Sanders,<sup>10</sup> all previous experiments have been performed at saturated vapor pressure below the  $\lambda$  point, which has limited the atomic density to  $1.6 \times 10^{22} \text{ cm}^{-3}$  in  ${}^3\text{He}$  and  $2.2 \times 10^{22} \text{ cm}^{-3}$

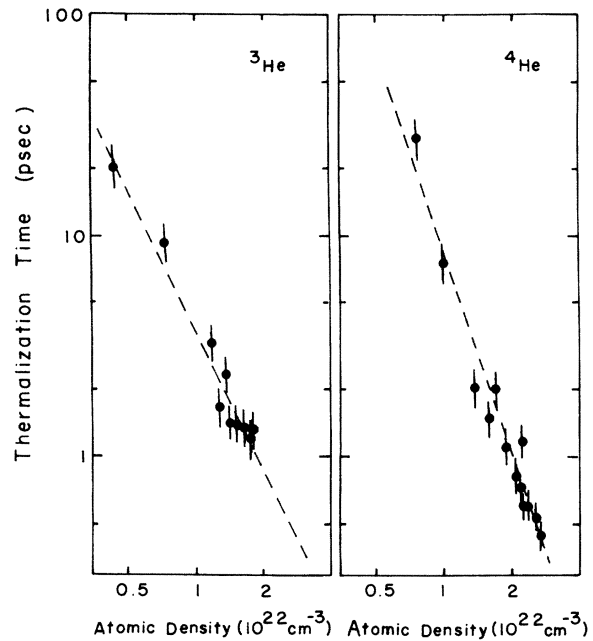


FIG. 4. Average thermalization time for injected hot electrons in  ${}^3\text{He}$  and  ${}^4\text{He}$  as a function of atomic density.

in  ${}^4\text{He}$ . Sommer<sup>6</sup> obtained a barrier of 1.3 eV by injection of field-driven electrons from the vapor into the liquid. Woolf and Rayfield<sup>7</sup> found a shift of 1.02 eV in the response of a phototube after it had been filled with liquid  ${}^4\text{He}$ . Schoepe and Rayfield<sup>8</sup> determined values of the binding energy of the electronic bubble state in  ${}^3\text{He}$  and  ${}^4\text{He}$  by electron tunneling through the liquid-vapor interface. From this they inferred barrier values of 0.82 and 0.65 eV for  ${}^4\text{He}$  and  ${}^3\text{He}$ , respectively. Northby and Sanders<sup>9</sup> and Zipfel and Sanders<sup>10</sup> found a density-dependent well depth for the  ${}^4\text{He}$  bubble state by studying photoexcitation of the bubble state in the liquid under pressure. An interpretation of their data by Miyakawa and Dexter<sup>26</sup> is given in terms of transitions between bound states within the bubble. They could not distinguish between the Wigner-Seitz or optical models on the basis of their calculations, although they suggest a well depth of 0.95 eV at zero pressure as consistent with their approach.

The most striking feature of the comparison of these results is that Sommer's single density value for the barrier falls within the range of our own density-dependent values, consistent with the Wigner-Seitz model. The barrier values from experiments employing bubble properties fall lower, closer to the theoretical values of the modified optical model. Since both Sommer's experiment and ours involve injection of electrons into the bulk fluid and do not explicitly depend on bubble-

TABLE I. Comparison of experimental barrier results.

Reference	Temperature (°K)	Pressure	Atomic density ( $10^{22}$ cm $^{-3}$ )	Barrier value (eV)
$^4\text{He}$				
7	1.1	SVP	2.2	1.02 <sup>a</sup>
6	<1.5	SVP	2.2	1.3 ± 0.4
10, 26	1.25	0 atm <sup>b</sup>	2.2	0.95 <sup>a</sup>
9	<1.7	SVP	2.2	1.0 ± 0.2
8	1.2–1.9	SVP	2.2	0.82 <sup>a</sup>
This research <sup>c</sup>	7.5	30 atm	2.3	1.2 ± 0.1
This research <sup>c</sup>	2.5	2 atm	2.2	1.1 ± 0.1
$^3\text{He}$				
8	0.65–1.1	SVP	1.6	0.65 <sup>a</sup>
This research <sup>c</sup>	2.2	4.6 atm	1.8	1.0 ± 0.1

<sup>a</sup> Authors state no limits of error.

<sup>b</sup> This is an extrapolation of experimental data to zero pressure.

<sup>c</sup> Figure 3 shows results over entire density range.

state parameters, it is possible that a detailed theoretical analysis of the different methods for finding  $E_B$  might reconcile this apparent disagreement.

## VI. SUMMARY

We have determined the density dependence of the electron surface barrier for  $^3\text{He}$  and  $^4\text{He}$  fluids, by injection of electrons from a planar gold surface. The barrier values agree, for both isotopes, with a Wigner-Seitz calculation of the barrier. Comparison with other theoretical calculations and experiments are carried out and suggest the pos-

sibility that the barrier values obtained for "bubble"-related experiments may differ from those obtained for electron injection through a planar surface. Further experiments and theoretical studies are indicated. Comparable results have been obtained in  $\text{H}_2$  and  $\text{D}_2$ ,<sup>27</sup> and are currently being analyzed in depth.

## ACKNOWLEDGMENTS

The authors wish to express their thanks to D. P. Goshorn and D. E. Freund of this Laboratory for experimental assistance. We also acknowledge helpful discussions with A. L. Fetter, H. Meyer, and G. T. McConville.

† Supported by National Science Foundation Grant No. GH-37278.

<sup>1</sup>B. Burdick, Phys. Rev. Lett. **14**, 11 (1965).

<sup>2</sup>J. L. Levine and T. M. Sanders, Jr., Phys. Rev. **154**, 138 (1967).

<sup>3</sup>A. L. Fetter, in *The Physics of Liquid and Solid Helium*, edited by K. H. Benneman and J. B. Ketterson (Wiley, New York, 1976).

<sup>4</sup>J. Jortner, N. R. Kestner, S. A. Rice, and M. H. Cohen, J. Chem. Phys. **43**, 2614 (1965).

<sup>5</sup>L. L. Tankersley, J. Low Temp. Phys. **2**, 451 (1973).

<sup>6</sup>W. T. Sommer, Phys. Rev. Lett. **12**, 271 (1964).

<sup>7</sup>M. A. Woolf and G. W. Rayfield, Phys. Rev. Lett. **15**, 235 (1965).

<sup>8</sup>W. Schoepe and G. W. Rayfield, Phys. Rev. A **7**, 2111 (1973).

<sup>9</sup>J. A. Northby and T. M. Sanders, Jr., Phys. Rev. Lett.

**18**, 1184 (1967).

<sup>10</sup>C. Zipfel and T. M. Sanders, Jr., in *Proceedings of the Eleventh International Conference on Low Temperature Physics*, edited by J. F. Allen, D. M. Finlayson, and D. M. McCall (St. Andrews University Press, St. Andrews, Scotland, 1968).

<sup>11</sup>David G. Onn and M. Silver, Phys. Rev. **183**, 295 (1969).

<sup>12</sup>David G. Onn and M. Silver, Phys. Rev. A **3**, 1773 (1971).

<sup>13</sup>P. Smejtek, M. Silver, K. S. Dy, and D. G. Onn, J. Chem. Phys. **59**, 1374 (1973).

<sup>14</sup>D. G. Onn, P. Smejtek, and M. Silver in *Proceedings of the Thirteenth International Conference on Low Temperature Physics, Boulder, Colo., 1972*, edited by W. J. O'Sullivan, K. D. Timmerhaus and E. F. Hammel (Plenum, New York, 1974); also D. G. Onn, P. Smejtek, and M. Silver, J. Appl. Phys. **45**, 199

- (1974).
- <sup>15</sup>CryoCal, Inc., Riviera Beach, Fla.
- <sup>16</sup><sup>3</sup>He (low <sup>4</sup>He content), Monsanto Chemical Co., Mound Laboratory, Miamisburg, Ohio; <sup>4</sup>He (research grade 99.9995%), Union Carbide Corp., Linde Div., Keasbey, N. J. 08832
- <sup>17</sup>Heise Bourdon Tube Co., Inc. Newtown, Conn.
- <sup>18</sup>R. D. McCarty, NBS Technical Note No. 631 (SD Cat. No. C13.46:631) (U.S. GPO, Washington, D.C., 1972).
- <sup>19</sup>R. H. Sherman and F. J. Edeskuty, *Ann. Phys.* **9**, 522 (1960).
- <sup>20</sup>W. E. Keller, *Helium-3 and Helium-4* (Plenum, New York, 1969), Chap. 3.
- <sup>21</sup>L. A. McColl, *Phys. Rev.* **56**, 699 (1939).
- <sup>22</sup>J. J. Thomson, *Conduction of Electricity Through Gases* (Cambridge U.P., London, 1928), 3rd ed., Vol. 1, p. 466; L. Loeb, *Basic Processes of Gaseous Electronics* (California U.P., Berkeley, Calif., 1955), Chap. VII.
- <sup>23</sup>T. F. O'Malley, *Phys. Rev.* **130**, 1020 (1963).
- <sup>24</sup>W. Legler, *Phys. Lett.* **A31**, 129 (1970).
- <sup>25</sup>James R. Broomall and David G. Onn, in *Proceedings of the Fourteenth International Conference on Low Temperature Physics*, edited by M. Krusius and M. Vuorio (North-Holland, Amsterdam, 1975).
- <sup>26</sup>T. Miyakawa and D. L. Dexter, *Phys. Rev.* **A1**, 513 (1970).
- <sup>27</sup>Wayne D. Johnson and David G. Onn, in *Proceedings of the Fourteenth International Conference on Low Temperature Physics*, edited by M. Krusius and M. Vuorio (North-Holland, Amsterdam, 1975).